Neural primacy of the dorsolateral prefrontal cortex in patients with obsessive-compulsive disorder

Hailong Li[a,b,1], Xinyu Hu[a,b,1], Yingxue Gao[a,b], Lingxiao Cao[a,b], Lianqing Zhang[a,b], Xuan Bu[a,b], Lu Lu[a,b], Yanlin Wang[a,b], Shi Tang[a,b], Bin Li[c], Yanchun Yang[c], Bharat B. Biswal[d,e], Qiyong Gong[a,b], Xiaoqi Huang[a,b,*]

[a] Huaxi MR Research Center (HMRRC), Department of Radiology, West China Hospital of Sichuan University, Chengdu, PR China
[b] Research Unit of Psychoradiology, Chinese Academy of Medical Sciences, Chengdu, PR China
[c] Department of Psychiatry, West China Hospital of Sichuan University, Chengdu, PR China
[d] Department of Biomedical Engineering, New Jersey Institute of Technology, Newark, NJ, USA
[e] The Clinical Hospital of Chengdu Brain Science Institute, MOE Key Laboratory for Neuroinformation, University of Electronic Science and Technology of China, Chengdu, PR China

ARTICLE INFO

ABSTRACT

The dorsolateral prefrontal cortex (DLPFC), a key structure in the executive system, has consistently emerged as a crucial element in the pathophysiology of obsessive–compulsive disorder (OCD). However, the neural primacy of the DLPFC remains elusive in this disorder. We investigated the causal interaction (measured by effective connectivity) between the DLPFC and the remaining brain areas using bivariate Granger causality analysis of resting-state fMRI collected from 88 medication-free OCD patients and 88 matched healthy controls. Additionally, we conducted seed-based functional connectivity (FC) analyses to identify network-level neural functional alterations using the bilateral DLPFC as seeds. OCD patients demonstrated reduced FC between the right DLPFC and right orbitofrontal cortex (OFC), and activity in the right OFC had an inhibitory effect on the right DLPFC. Additionally, we observed alterations in both feedforward and reciprocal influences between the inferior temporal gyrus (ITG) and the DLPFC in patients. Furthermore, activity in the cerebellum had an excitatory influence on the right DLPFC in OCD patients. These findings may help to elucidate the psychopathology of OCD by detailing the directional connectivity between the DLPFC and the rest of the brain, ultimately helping to identify regions that could serve as treatment targets in OCD.

1. Introduction

Obsessive-compulsive disorder (OCD), a disabling disorder that affects approximately 2–3% of the population, is characterized by recurrent and persistent impulses (obsessions) and repetitive behaviors (compulsions) (Milad and Rauch, 2012; Stein et al., 2019). Although significant progress has been made in understanding OCD with the rapid development of neuroscience techniques, the exact neural pathophysiology of this disorder is still unclear (Dougherty et al., 2018; Robbins et al., 2019; Stein et al., 2019).

Several recent studies have noted that abnormality of the dorsolateral prefrontal cortex (DLPFC) is closely related to symptomatic features of OCD, including excessive doubt and repetitive actions

(Abramowitz et al., 2009; Mataix-Cols et al., 2003; Russell et al., 2003; Schmidtke et al., 1998). The DLPFC has been the most investigated target for noninvasive neuromodulatory treatment in OCD (Shivakumar et al., 2019). Evidence from recent meta-analyses indicated that repeated transcranial magnetic stimulation (rTMS) targeting the left, right, or bilateral DLPFC was significantly more effective than sham rTMS in improving OCD symptoms (Lusicic et al., 2018; Rehn et al., 2018; Zhou et al., 2017). In addition, the activation of the DLPFC during symptom provocation tasks was negatively correlated with the response to cognitive behavioral therapy (CBT), which indicated that excessive activation of the DLPFC may hinder the response to CBT (Olatunji et al., 2014). Nevertheless, the exact neural mechanism of the DLPFC in OCD remains to be clarified.

Several lines of evidence from structural and functional neuroimaging studies have reinforced the crucial role of the DLPFC in the pathophysiology of OCD. Both the volume and the thickness of the DLPFC were found to be reduced in OCD patients relative to healthy controls (Boedhoe et al., 2018; de Wit et al., 2014). Task-based fMRI studies employing cognitive and executive tasks indicated decreased responsiveness of the DLPFC during the planning task in OCD patients (Menzies et al., 2008; van den Heuvel et al., 2005), and hyperactivation of the DLPFC during working memory performance was associated with improved task performance (de Vries et al., 2014; Nakao et al., 2009). In prior resting-state FC studies, dysconnectivity concerning the DLPFC has been identified in patients with OCD through rs-fMRI (Anticevic et al., 2014; Gursel et al., 2018; Vaghi et al., 2017) with both whole-brain and ROI-restricted analyses. Specifically, a recent meta-analysis of seed-based resting-state FC studies has provided evidence that both hypoconnectivity within the frontoparietal network (FPN) and dysconnectivity between the default-mode network (DMN), salience network (SN), limbic network (LN) and FPN are anchored in the DLPFC in OCD patients (Gursel et al., 2018).

The brain is a complex network of interconnected regions (Bressler and Menon, 2010), and these regions interact with each other through brain connectivity, producing an integrated outcome that determines the symptoms (Bressler and Menon, 2010; Friston, 2011; Tang et al., 2017). Thus, exploring the neural primacy of the DLPFC—or, to be more exact, how DLPFC activity drives the activity of other regions and whether there are alterations in feedback mechanisms from other brain regions to the DLPFC—can help us better understand the pathophysiology of OCD. However, given the critical role of the DLPFC in OCD pathology, little is known about this specific causal effect of the DLPFC with other brain regions. In order to answer these questions, it is necessary to analyze the proposed causal interaction and directionality of influence between the DLPFC and other regions.

Granger causality analysis (GCA) aims to define causal effects by analyzing whether the preceding neural activity in one seed region predicts activity in another subsequent region (Friston, 2011; Hamilton et al., 2011; Palaniyappan et al., 2013; Tang et al., 2017), a phenomenon also known as effective connectivity (EC). Thus, GCA is a good choice for measuring EC between different brain regions and has been widely used to analyze blood-oxygen-level-dependent (BOLD) data in relation to psychiatric disorders, such as major depressive disorder (MDD) (Hamilton et al., 2011; Rolls et al., 2018) and schizophrenia (Jiang et al., 2018; Palaniyappan et al., 2013). Evidence from (Schippers et al., 2011) demonstrated that GCA accurately revealed causal influence in the vast majority of fMRI cases in group studies.

Previous studies on OCD revealed abnormal EC between the frontal region and the amygdala (Curcic-Blake et al., 2012) as well as the cingulate cortex (Schlosser et al., 2010) using task fMRI. In particular, hyperactivation of the DLPFC may lead to reduced top-down input to the OFC in OCD patients (Han et al., 2016); however, no study has explored the EC with a focus on the DLPFC using resting-state fMRI. Therefore, in the current study, we aimed to investigate whether the DLPFC produces aberrant neural information flow in adult OCD patients. We hypothesized that EC alterations would occur between the DLPFC and OFC in task-free conditions. We also performed conventional seed-based whole-brain correlation analysis of the resting-state functional connectivity (rsFC) of the DLPFC. Finally, we investigated whether abnormal FC or EC was associated with clinical symptom severity and illness duration.

2. Materials and methods

2.1. Participants

A total of eighty-eight medication-free OCD patients were recruited from the Mental Health Center, West China Hospital of Sichuan University. The diagnosis of OCD was determined by consensus between two experienced psychiatrists by using the Structured Clinical Interview for DSM-IV (SCID)–Patient Version. The exclusion criteria were (i) pregnancy, (ii) any history of major physical disease such as cardiovascular disease or neurological disorder, (iii) pharmacotherapy or psychotherapy within one month of the MRI data collection, (iv) substance dependence or abuse and (v) age under 18 or over 60 years.

We applied the Yale–Brown Obsessive Compulsive Scale (Y-BOCS) to evaluate the severity of OCD symptoms. Additionally, the OCD patients used the 14-item Hamilton Anxiety Rating Scale (HAMA) and the 17-item Hamilton Depression Rating Scale (HAMD) to rate the severity of their anxious and depressive symptoms, respectively. Seventy-four patients were medication naive, and the remaining fourteen had received medication previously (clomipramine in four, paroxetine in three, fluoxetine in three, sertraline in three, and quetiapine in one). All the patients completed a washout period of at least four weeks before MRI data acquisition. Eighty-eight healthy controls (HCs) were recruited from the local region through advertising posters and screened with the SCID–Non-Patient Version to confirm the absence of neurological and mental disorders.

The Ethics Committee of the West China Hospital of Sichuan University approved the current research, and each participant provided written informed agreement before the investigation procedure was initiated.

2.2. Image acquisition

OCD patients and HCs underwent scanning using a 3.0 T GE Signa EXCITE MRI scanner equipped with an 8-channel head coil. During MRI data acquisition, each subject was instructed to stay awake and keep his or her eyes closed. All participants were asked to complete a resting-state scanning questionnaire to ensure that they did not fall asleep during the scanning. Additionally, we used foam pads to protect the participants from scanner noise and minimize head motion. We utilized gradient-echo echo-planar imaging to obtain MRI data sensitized to alterations in BOLD signal levels. The parameters for fMRI data acquisition were as follows: repetition time (TR)/echo time (TE) = 2000/30 ms, flip angle = 90°, slice thickness = 5 mm with no gap, 30 axial slices, 200 volumes in each run, field of view = 240 × 240 mm^2, and voxel size = 3.75 × 3.75 × 5 mm^3. A high-resolution 3-dimensional (3D) T1-weighted spoiled gradient recall sequence was used with the following parameters: TR/TE = 8.5/3.4 ms, flip angle = 12°, slice thickness = 1.0 mm, 156 contiguous coronal slices, and field of view = 240 × 240 mm^2.

2.3. Image preprocessing

In the present investigation, we applied DPABI software (Yan et al., 2016) for the image preprocessing procedures, which included slice timing, head-motion correction, and normalization (voxel size 3 × 3 × 3 mm^3) to the Montreal Neurological Institute (MNI) space. The first ten time points were discarded to ensure signal stabilization. The data were realigned to the first volume to correct head motion. To remove the head-motion artifacts, we adopted the regressors of the Friston 24-parameter model, which has been demonstrated to be superior to the 6-parameter model (Yan et al., 2013). Furthermore, we regressed out covariates including cerebrospinal fluid signal, white matter signal, and global mean intensity to minimize the effects of nonneuronal BOLD fluctuations. Afterwards, the linear trend of the rs-fMRI data was removed, and bandpass filtering (0.01–0.08 Hz) was conducted to minimize the effect of high-frequency physiological noise and extreme low-frequency drift.

2.4. Quality control for head motion

We used stringent criteria to minimize the effects of head motion on FC and EC. The motion correction strategies suggested by previous

studies (Power et al., 2013; Yan et al., 2013) proposed mean framewise displacement (FD) < 0.2 mm as the threshold for inclusion criteria to minimize the effects of head motion on BOLD fMRI studies. This method brings about a great reduction in motion-induced artifacts when combined with various motion correction strategies (Power et al., 2013; Satterthwaite et al., 2013). This threshold has been widely used in recent studies to rigorously control head motion (Fukushima et al., 2018; Hilger and Fiebach, 2019; Yan et al., 2019). Mean FD values were calculated from translational and rotational scan-to-scan displacements using three translational parameters and three rotational parameters obtained from realignment steps for each subject (Power et al., 2013). The rs-fMRI images met the criteria of < 1.5 mm of spatial movement and < 1.5 degrees of rotation in any direction and a mean FD value < 0.2 mm. According to these criteria, no subject was excluded in either the OCD group or the HC group.

2.5. Selection of the seed regions

The bilateral DLPFC seeds were defined as spheres with a 6-mm radius, centered at the MNI coordinates (x = ± 56, y = 26, z = 25) (Stein et al., 2007). According to the referenced study, the coordinates of the DLPFC seeds were determined based on previous knowledge of its interaction in an emotional network and the coordinates with the highest activation of FC with the amygdala (Meyer-Lindenberg et al., 2005; Pezawas et al., 2005).

2.6. EC analysis

We used GCA to identify the causal influences between the DLPFC and other brain regions in OCD patients. Bivariate signed-path coefficient-based voxelwise Granger causality analysis was conducted using REST-GCA software (http://www.restfmri.net/forum, version 1.8) (Zang et al., 2012). According to the principle of GCA, one time series (X) is defined to have a causal effect on another time series (Y) if the preceding neural activity of X uniquely predicts the activity of Y relative to what the preceding neural activity of Y can predict itself (Hamilton et al., 2011; Seth et al., 2015). The signed-path coefficient is estimated to infer the possible inhibitory or excitatory effects of the directed influence. A positive path coefficient may imply excitatory influence, and a negative coefficient may be defined as a sign of inhibitory influence (Guo et al., 2015; Palaniyappan et al., 2013).

2.7. FC analysis

The Resting-State fMRI Data Analysis Toolkit (REST) (http://www.restfmri.net/forum, version 1.8) was then used to calculate FC. Seed-based resting-state FC analysis of the bilateral DLPFC was performed. Pearson's correlation coefficients were computed between the mean time course of the DLPFC and each voxel of the whole brain. The voxelwise Pearson's correlation coefficients were then converted to Z-scores using Fisher's Z transform for further statistical analysis.

2.8. Statistical analysis

Within-group FC and EC patterns were evaluated using a one-sample t-test for each group separately. Then, group differences in FC and EC patterns were compared by using a two-sample t-test. We regressed out confounding covariates, including gender, age, and mean FD values, in all group-level analyses. Neuroimaging statistical analyses utilized a statistical height threshold of p < 0.001 (uncorrected) at the voxel level and a familywise error (FWE) correction (p < 0.05) at the cluster level. All statistical analyses were carried out using SPM8 software (http://www.fil.ion.ucl.ac.uk/spm/software/spm8/).

Table 1
Demographic and clinical characteristics of participants.

| Characteristic | OCD (n = 88) | | HC (n = 88) | | Significance |
	Mean	SD	Mean	SD	P Value
Gender (Male: Female)	56:32	–	56:32	–	1.000
Age (Years)	29.16	8.71	27.88	10.58	0.38
Education (Years)	13.91	2.88	–	–	–
Duration of Illness (Years)	7.32	5.58	–	–	–
Y-BOCS Total	21.51	5.37	–	–	–
Obsessions	13.14	5.05	–	–	–
Compulsions	8.37	5.34	–	–	–
HAMD-17	8.74	4.921	–	–	–
HAMA-14	8.78	4.46	–	–	–
Current Treatment Status	**n**	**%**	**–**	**–**	**–**
Drug Free (> 4 Weeks)	88	100	–	–	–
Medication Naive	74	88.09	–	–	–
Previous Treatment History	**n**	**%**	**–**	**–**	**–**
Clomipramine	4	4.55	–	–	–
Paroxetine	3	3.41	–	–	–
Fluoxetine	3	3.41	–	–	–
Sertraline	3	3.41	–	–	–
Quetiapine	1	1.14	–	–	–

Abbreviations: HAMA, Hamilton Anxiety Rating Scale; HAMD, Hamilton Depression Rating Scale; HC, healthy control; OCD, obsessive–compulsive disorder; SD, standard deviation; Y-BOCS, Yale-Brown Obsessive Compulsive Scale.

2.9. Correlation with symptom severity and duration

Correlations with symptom severity and illness duration were examined by extracting FC Z scores and GCA coefficients separately from regions showing group differences and correlating these values with Y-BOCS scores, HAMA scores, HAMD scores and duration of illness in the OCD group. The p values were corrected for multiple comparisons using the Bonferroni correction.

3. Results

3.1. Demographic and clinical characteristics

The demographic and clinical characteristics of the two groups are presented in Table 1. For the 88 OCD patients, the total Y-BOCS score was 21.51 ± 5.37, corresponding to moderate or severe OCD symptoms, with obsessive and compulsive subscale scores of 13.14 ± 5.05 and 8.37 ± 5.34, respectively. The duration of OCD symptoms was 7.32 ± 5.58 years. The HAMA score was 8.78 ± 4.46, and the HAMD score was 8.74 ± 4.92, indicating mild depression.

3.2. EC patterns

Within-group EC patterns: In HCs, we observed bidirectional communication between the left DLPFC and the posterior cingulate cortex (PCC). The left DLPFC exerted an inhibitory influence on the PCC, whereas the PCC had an excitatory influence on the left DLPFC. The left DLPFC had an inhibitory influence on the precuneus and an excitatory influence on the inferior frontal gyrus and amygdala. The supplementary motor area (SMA) had an excitatory influence on the left DLPFC. The right DLPFC had an inhibitory influence on the SMA and an excitatory influence on the right inferior temporal gyrus (ITG). The OFC had an excitatory influence on the right DLPFC (Supplementary Fig. 1).

In the OCD group, the left DLPFC had an inhibitory influence on the SMA and an excitatory influence on the amygdala and middle temporal gyrus. The right inferior parietal lobule (IPL) had an excitatory influence on the left DLPFC. The right DLPFC had an inhibitory influence on the SMA and an excitatory influence on the bilateral ITG, while the bilateral ITG had an inhibitory influence on the right DLPFC (Supplementary Fig. 1).
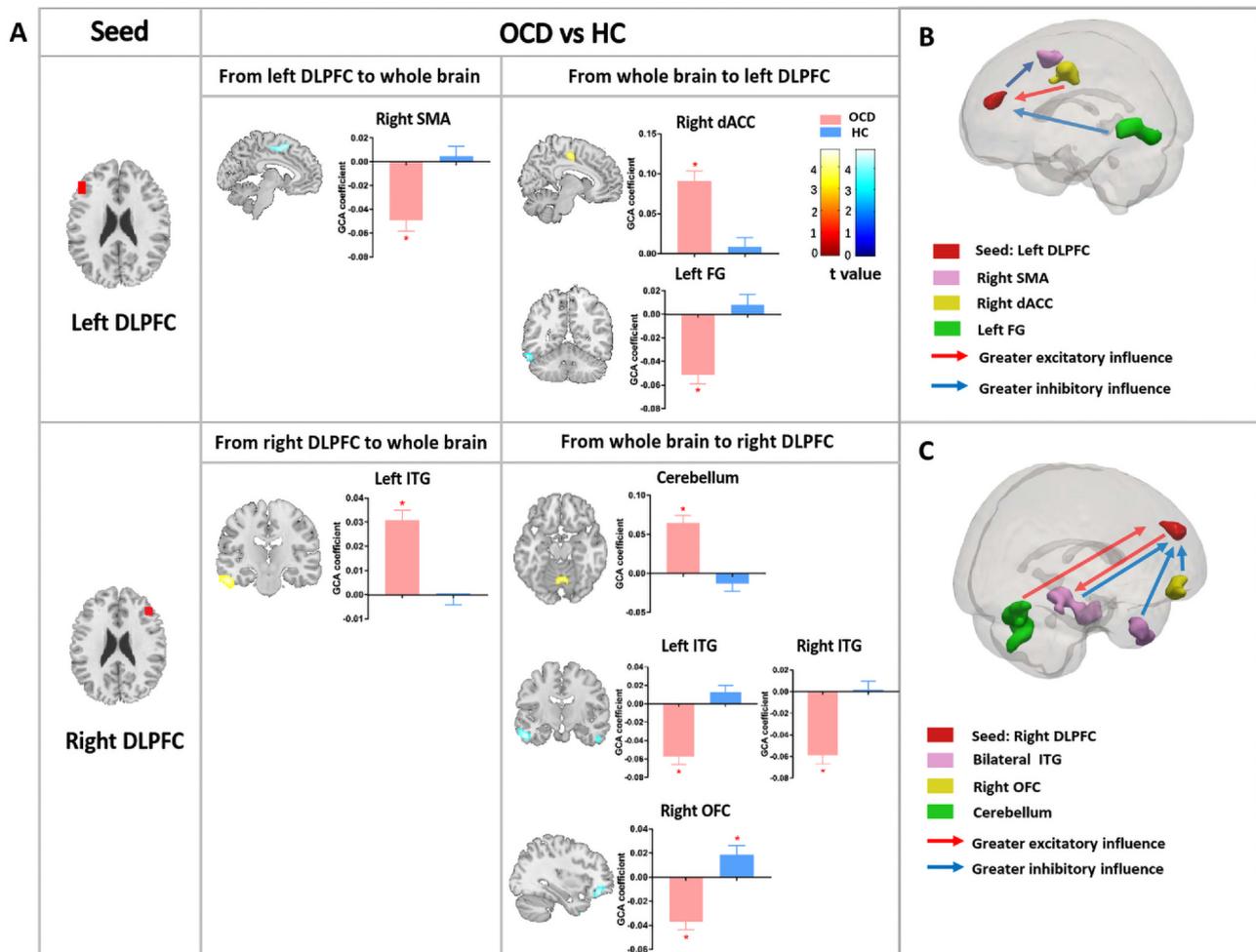
Fig. 1. Group differences in effective connectivity. (A) The figure shows the group differences in EC from the bilateral DLPFC to the whole brain and from the whole brain to the bilateral DLPFC. Each bar reflects the mean GCA coefficient of the corresponding group; error bars represent the standard error of the mean. Asterisks indicate that the mean GCA coefficients are significantly different from zero. Color bars represent t values from the between-group t-tests; warm/cold colors denote significantly greater excitatory/inhibitory influence in OCD patients than in HCs. (B) Schematic representation of group differences in causal influence on and by the left DLPFC in OCD patients compared to controls; red/blue arrows indicate significantly greater excitatory/inhibitory influence in OCD patients than in HCs. (C) Schematic representation of group differences in causal influence on and by the right DLPFC in OCD patients compared to controls; red/blue arrows indicate significantly greater excitatory/inhibitory influence in OCD patients than in HCs. Abbreviations: EC, effective connectivity; DLPFC, dorsolateral prefrontal cortex; GCA, Granger causality analysis; HC, healthy control; SMA, supplementary motor area; dACC, dorsal anterior cingulate cortex; FG, fusiform gyrus; ITG, inferior temporal gyrus; OFC, orbitofrontal cortex; HAMA, Hamilton Anxiety Rating Scale. (For interpretation of the references to color in this figure legend, the reader is referred to the web version of this article.)

Between-group EC patterns: The bivariate left-DLPFC-to-whole-brain analysis showed that the left DLPFC had an inhibitory influence on the SMA in OCD patients [OCD: $t_{(87)} = -5.396$, $p < 0.001$], while the controls showed no significant causal influence from the left DLPFC to the SMA [HC: $t_{(87)} = 0.559$, $p = 0.578$]. The whole-brain-to-left-DLPFC analysis showed that the left dorsal anterior cingulate cortex (dACC) had an excitatory influence on the left DLPFC only in OCD patients [OCD:

$t_{(87)} = 7.362$, $p < 0.001$; HC: $t_{(87)} = 0.730$, $p = 0.468$]. The left fusiform gyrus (FG) also had an inhibitory influence on the left DLPFC only in OCD patients [OCD: $t_{(87)} = -6.301$, $p < 0.001$; HC: $t_{(87)} = 0.903$, $p = 0.369$] (Fig. 1, Table 2).

The right-DLPFC-to-whole-brain analysis showed that the right DLPFC had an excitatory effect on the left ITG only in OCD patients [OCD: $t_{(87)} = 7.664$, $p < 0.001$; HC: $t_{(87)} = 0.014$, $p = 0.989$]. Furthermore, whole-brain-to-right-DLPFC analysis noted that activation in the cerebellum had an excitatory influence on the right DLPFC only in OCD patients [OCD: $t_{(87)} = 6.461$, $p < 0.001$; HC: $t_{(87)} = -1.336$, $p = 0.185$]. We also observed that the right OFC had an inhibitory

influence on the right DLPFC in OCD patients [OCD: $t_{(87)} = -5.396$, $p < 0.001$], while the right OFC had an excitatory influence on subsequent right DLPFC activity in HCs [HC: $t_{(87)} = 2.447$, $p = 0.016$]. The bilateral ITG had an inhibitory influence on the right DLPFC only in OCD patients [OCD: left ITG: $t_{(87)} = -6.754$, $p < 0.001$, right ITG: $t_{(87)} = -7.169$, $p < 0.001$; HC: left ITG: $t_{(87)} = 1.681$, $p = 0.096$, right ITG: $t_{(87)} = 0.2495$, $p = 0.804$] (Fig. 1, Table 2).

3.3. FC patterns

Within-group FC patterns: A one-sample *t*-test of FC maps reflecting functional coupling between the DLPFC and the rest of the brain revealed a significant positive correlation between the left DLPFC and the ITG, IPL, and inferior frontal gyrus in both OCD and healthy control groups. A significant negative correlation was found between the bilateral DLPFC and the occipital lobe, precuneus, cingulate cortex, prefrontal cortex, cerebellum, precentral gyrus and postcentral gyrus (Supplementary Fig. 2).

Between-group FC patterns: A two-sample *t*-test comparing the FC

Table 2
Between-group differences in the causal influences from and to the bilateral DLPFC.

Cluster Location	MNI Coordinates (x, y, z)	Mean (SE) GCA Coefficient in HC Group	Mean (SE) GCA Coefficient in OCD Group	Cluster Size	t Value	p-FWE
Causal Influence of Left DLPFC on Whole Brain						
Right Supplementary Motor Area	3, 3, 54	0.005(0.008)	−0.049(0.009)	131	−3.91	0.035
Causal influence of Whole Brain on Left DLPFC						
Right Dorsal Anterior Cingulate Cortex	7, −12, 49	0.009(0.012)	0.091(0.012)	125	5.08	0.025
Left Fusiform Gyrus	−63, −42, −18	0.008(0.009)	−0.051(0.008)	143	−4.72	0.015
Causal Influence of Right DLPFC on Whole Brain						
Left Inferior Temporal Gyrus	−57, −15, −27	−0.001(0.004)	0.031(0.004)	246	4.67	0.007
Causal Influence of Whole Brain on Right DLPFC						
Cerebellum	−18, −57, −21	−0.013(0.010)	0.065(0.010)	411	4.58	< 0.001
Right Orbitofrontal Cortex	33, 39, −15	0.019(0.008)	−0.037(0.007)	99	−4.66	0.038
Left Inferior Temporal Gyrus	−42, 6, −45	0.013(0.007)	−0.057(0.008)	304	−4.79	< 0.001
Right Inferior Temporal Gyrus	45, 12, −45	0.002(0.008)	−0.059(0.008)	164	−4.36	0.005

*Positive t values represent OCD > HC; negative t values represent OCD < HC.
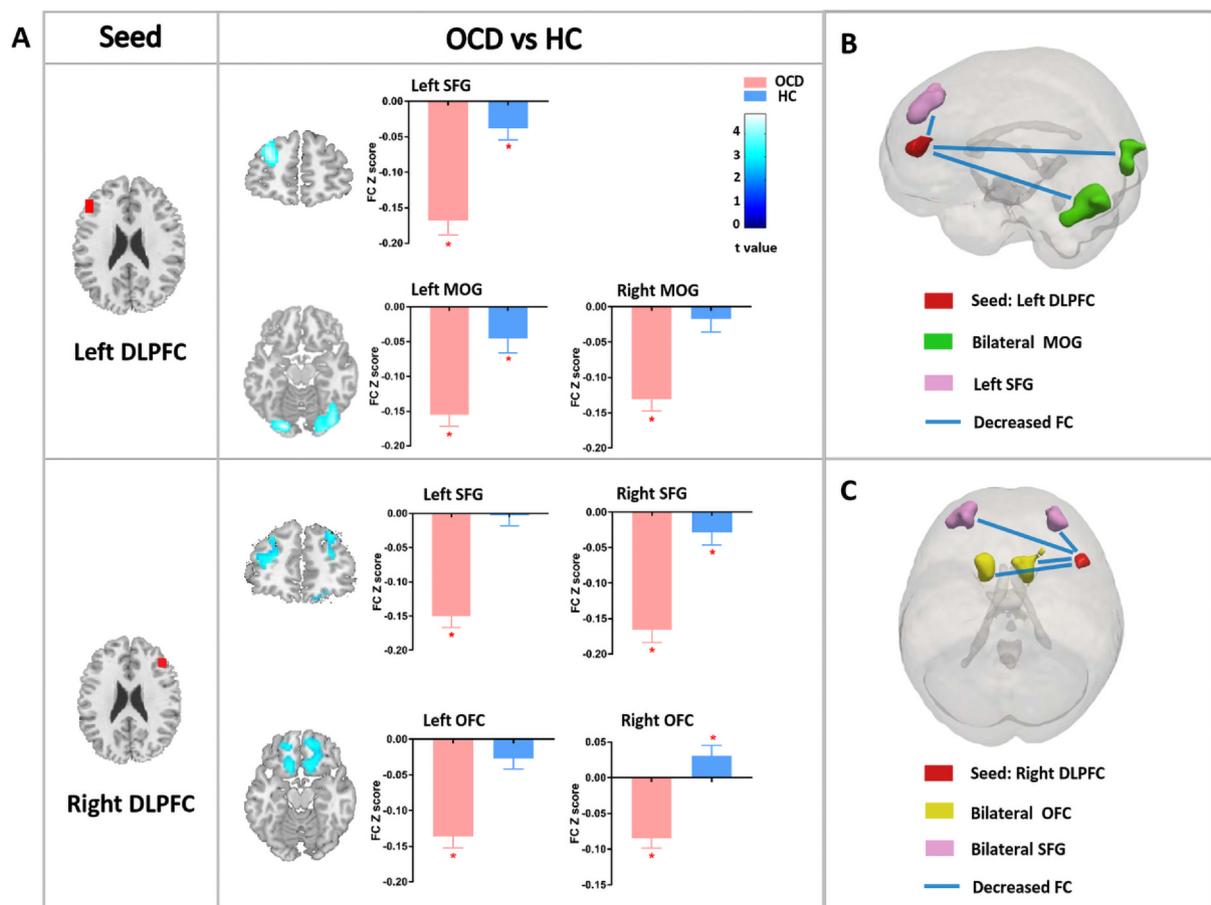
Fig. 2. Group differences in functional connectivity. (A) The figure shows the group differences in FC between the bilateral DLPFC and the whole brain. Each bar reflects the mean FC Z score of the corresponding group, error bars represent standard errors of the means. Asterisks indicate that the mean FC Z scores are significantly different from zero. Color bars represent t values from the between-group t-test, warm/cold color indicates increased/decreased FC in OCD patients compared to HCs. (B) Schematic representation of the left-DLPFC-based FC pattern in OCD patients compared to HCs; blue/red arrows indicate significantly decreased/increased FC in OCD patients compared to HCs. (C) Schematic representation of the right-DLPFC-based FC pattern in OCD patients compared to HCs; blue/red arrows indicate significantly decreased/increased FC in OCD patients versus controls. Abbreviations: FC, functional connectivity; DLPFC, dorsolateral prefrontal cortex; OCD, obsessive–compulsive disorder; HC, healthy control; SFG, superior frontal gyrus; MOG, middle occipital gyrus; OFC, orbitofrontal cortex; Y-BOCS, Yale–Brown Obsessive Compulsive Scale. (For interpretation of the references to color in this figure legend, the reader is referred to the web version of this article.)

maps of OCD patients and HCs revealed significantly decreased FC between the left DLPFC and left superior frontal gyrus (SFG) and between the left DLPFC and bilateral middle occipital gyrus (MOG) in OCD patients compared with HCs. We also observed decreased FC between the right DLPFC and bilateral OFC in the OCD group. Furthermore, patients showed significantly decreased FC between the right DLPFC and bilateral SFG (Fig. 2, Table 3).

3.4. Correlation with symptom severity and duration

None of the correlations survived Bonferroni correction for multiple comparisons. As an exploratory correlation analysis, we present the

Table 3
Between-group differences in the functional connectivity (FC) between the bilateral DLPFC and the whole brain.

Cluster Location	MNI Coordinates (x, y, z)	Mean (SE) FC Coefficient in HC Group	Mean (SE) FC Coefficient in OCD Group	Cluster Size	t Value	p-FWE
Between Left DLPFC and Whole Brain						
Right Middle Occipital Gyrus	30, −87, −9	−0.017(0.019)	−0.131(0.017)	356	−4.53	0.001
Left Middle Occipital Gyrus	−21, −87, −15	−0.046(0.021)	−0.155(0.017)	140	−4.52	0.035
Left Superior Frontal Gyrus	−21, 45, 15	−0.039(0.016)	−0.168(0.020)	174	−4.24	0.017
Between Right DLPFC and Whole Brain						
Left Superior Frontal Gyrus	−24, 51, 15	−0.003(0.015)	−0.150(0.016)	419	−6.02	< 0.001
Right Superior Frontal Gyrus	33, 42, 45	−0.029(0.018)	−0.166(0.018)	393	−5.30	< 0.001
Left Orbitofrontal Cortex	−15, 21, −18	−0.027(0.015)	−0.136(0.016)	186	−4.83	0.013
Right Orbitofrontal Cortex	12, 51, −12	0.031(0.015)	−0.085(0.013)	391	−4.44	< 0.001

*Positive t values represent OCD > HC; negative t values represent OCD < HC.

correlation results using nominal significance thresholds (p < 0.05, uncorrected) in Supplementary Fig. 3.

4. Discussion

OCD has been regarded as a "model" psychiatric disorder for neuroscience researchers, with broader relevance to the understanding of many other psychiatric disorders (Robbins et al., 2019). In this study, we investigated the neural primacy of the DLPFC in patients with OCD using rs-fMRI and found dysfunction in the DLPFC-OFC circuit, DLPFC-ITG circuit and DLPFC-cerebellum circuit, supporting alternative models for dysfunction of neural circuits in OCD patients (Stein et al., 2019). First, we found that, compared to HCs, OCD patients had a decreased negative correlation between the right DLPFC and right OFC, and the right OFC had an inhibitory effect on the right DLPFC; these regions constitute the DLPFC-OFC circuit. Second, in OCD patients, we observed failure in both feedforward and reciprocal influences between the ITG and the DLPFC, which constitute the DLPFC-ITG circuit. Third, the significant alterations in the causal influence of the cerebellum on the DLPFC in OCD patients provide evidence for a breakdown of the DLPFC-cerebellum circuit in the executive control deficit that characterizes OCD.

We combined the EC and FC analyses to explore the causal interactions and functional coupling between the DLPFC and other individual regions of the whole brain. We found that the regions showing EC with the DLPFC differed from those showing FC to the DLPFC, with the exception of the OFC, which showed decreased FC with and an inhibitory influence on the DLPFC. Thus, we concluded that the EC and FC analyses provide two different patterns of altered connectivity in OCD. The EC pattern confirmed the abnormal interactions between the DLPFC and multiple brain regions involved in large-scale networks, including the LN, DMN, SN and sensorimotor network (SMN), while the FC pattern demonstrated decreased functional correlations between the DLPFC and the SFG, MOG and OFC in OCD.

The human OFC exhibits reciprocal connections with the DLPFC derived from the lower bank and ventral part of the principal sulcus, as well as a close association with the rostral and lateral granular layer of the OFC in the human brain (Zald and Kim, 1996). The interaction of those two regions is vital in normal associative learning, and the disruption of their dynamic balance may be responsible for the pathophysiology associated with psychiatric disorders (Moghaddam and Homayoun, 2008).

In the current study, we observed a decreased functional correlation between the DLPFC and OFC in OCD patients compared to HCs, and activity in the OFC had an inhibitory effect on the right DLPFC in OCD. Meanwhile, the FC between the DLPFC and OFC was positively associated with obsession scores, suggesting a trend in which increasing severity of obsession reflects enhancement of negative functional connection between the DLPFC and OFC in OCD patients. Both the DLPFC and OFC are located in the PFC, which is involved in executive function, cognitive behavior, and regulation of self-control (Han et al., 2016;

Kwon et al., 2009; Savage et al., 1999). Notably, a previous task-induced EC study that administered a working memory task under emotional distraction revealed that hyperactivation of the DLPFC may lead to reduced top-down input to the OFC in OCD patients (Han et al., 2016). In light of that report combined with our own findings, which demonstrated that the OFC had an inhibitory effect on the right DLPFC in the resting state, we postulate that the OFC is a major inhibitor of the self-control function of the DLPFC in OCD patients in the resting state, while the DLPFC engages top-down control input to the OFC when emotional task stimulation is applied. This finding suggests that there may be a role shift between the DLPFC and OFC during task-performing and task-free states in patients with OCD.

In OCD patients, an abnormal DLPFC-ITG circuit was demonstrated in the form of an excitatory influence of the right DLPFC on the bilateral ITG, with the bilateral ITG providing inhibitory feedback to the right DLPFC. However, only an excitatory influence from the right DLPFC to the right ITG existed in HCs. The ITG is abnormally activated in OCD patients with compulsive checking (Phillips et al., 2000), and its activation is strongly associated with improved treatment response (Olatunji et al., 2014). With respect to the relationship between the DLPFC and ITG, a neurobiological model of visual working memory operations in humans has been identified based on the activation of object representations in the ITG via top-down feedback from the cortical area in the DLPFC to facilitate the maintenance and recoding of complex information (Ranganath, 2006). Our findings support the existence of the top-down excitatory effect from the DLPFC to the ITG in healthy people but not in OCD patients, even in the resting state. Thus, we proposed that the normal top-down feedback from the DLPFC to the ITG is perturbed in OCD patients.

Recent studies have begun to indicate that the cerebellum might be directly involved in the pathophysiology of OCD. OCD patients had increased gray matter volume in the cerebellar region, which has been confirmed by multicenter mega-analysis of voxel-based morphometry (VBM) studies (de Wit et al., 2014). Functional abnormalities of the cerebellum in OCD patients include decreased cerebellum-cerebral FC in executive control and emotional processing networks in the resting state (Xu et al., 2019) and reduced activation in the cerebellum during the cognitive control task state (Nabeyama et al., 2008). A global rs-fMRI study exhibited increased global brain connectivity in the cerebellum that correlated with OCD symptom severity (Anticevic et al., 2014). In addition, the cerebellum exhibited structural and functional connections to the cortico-striato-thalamo-cortical (CSTC) pathways, and the cerebellum has been thought to integrate the information flow of the CSTC circuit in patients with OCD (Middleton and Strick, 2000b). A recent view of the cerebellum holds that this region is not only involved in motor function but also crucial in executive control function. Evidence from diffusion tensor MRI studies has identified prefrontal cortex-cerebellar connections through the cortico-ponto-cerebellar and cerebello-thalamo-cortical pathways in both humans and nonhuman primates (Kelly and Strick, 2003; Middleton and Strick, 2000a; Ramnani, 2006; Stoodley, 2012). The cortico-pontine fibers from the

PFC converge in the cerebral peduncle on their way to the pontine nuclei, and then the pontine nuclei project to the cerebellum through the pontine-cerebellar fibers. In addition, the cerebellum returns projections to the PFC through the thalamus.

Our results provide the first evidence for the abnormal interaction between the cerebellum and DLPFC by showing that the cerebellum has an excitatory influence on the DLPFC in the FPN in patients with OCD. A previous rs-fMRI study showed functional correlations between the DLPFC and both Crus I and Crus II of the cerebellum in healthy people (Krienen and Buckner, 2009). These findings lend support to the view that the cerebellum processes executive control information from the DLPFC in the human brain. Our study clarified that the cerebellum had an excitatory influence on the DLPFC in OCD patients, which was not shown in HCs. We postulate that the regular inhibitory function of the brain is disrupted due to the overactivity of the cerebellum, further exciting the executive function of the DLPFC and finally resulting in compulsion symptoms in OCD.

Regarding the network-level hypothesis of neural dysfunction in OCD, we infer that patients with OCD have significant inhibitory neural influence from the DLPFC, which is a key node in the executive control system, to the OFC, a crucial node in the LN. In addition, the DLPFC, a node within the FPN, has an excitatory influence primarily on the ITG nodes of the DMN. The SN, anchored in the dACC, has an excitatory effect on the DLPFC. Furthermore, there is a significant abnormality in the influences on and by the DLPFC in patients with OCD regarding the nodes of the SMN, such as the SMA. Previous studies suggested that the SMA had increased relative activation during response inhibition (de Wit et al., 2012; Del Casale et al., 2011) and that hyperactivity of SMA was related to deficient inhibitory control, which may explain compulsions such as repetitive or ritualized behaviors in OCD patients (Rehn et al., 2018; Yucel et al., 2007). Our findings indicated that the DLPFC had an increased inhibitory influence on the SMA in patients with OCD, and the DLPFC may counteract SMA hyperactivity with feedback inhibition in OCD patients.

Evidence from a meta-analysis of resting-state FC revealed hypoconnectivity between the FPN, DMN, and SN. General dysconnectivity between the FPN and DMN, SN, and LN was consistently found in OCD studies (Gursel et al., 2018). Our observations confirm that the interaction between the DLPFC in the FPN and regions in the LN, DMN, SN, and SMN is significantly disrupted in OCD because the overactivity of the DLPFC in the FPN activates neural activity in DMN nodes and inhibits the activity of the SMN. In addition, the activity of the DLPFC in the FPN is under inhibitory control from the LN node, and the FPN is excited by the nodes of the SN, DMN and SMN.

One of the criticisms of GCA is that in some cases, the interregional differences in directionality could be due to systematic differences in hemodynamics between regions (or voxels). Because the fMRI signal represents a convolution of neuronal activity with the hemodynamic response function, the observed signal during rest (and also during tasks) represents a delayed signal due to the hemodynamic response. Thus, GCA between two regions in a subject may have been dominated by the underlying differences in the hemodynamic response function, independent of any neural differences. In the present study, we compared the GCA results of OCD patients and HCs during rest and found significant differences in the DLPFC, OFC, and ITG. To the best of our knowledge, there are no known differences in the underlying hemodynamic response function between OCD subjects and HCs. There are also no known studies have shown vascular differences between the two groups. In particular, there are no known vascular differences in the DLPFC, OFC, or other regions between OCD patients and HCs. Additionally, for this study, GCA was performed in 1000 bootstrap replicates and the results were highly reliable and similar to those obtained using the full original dataset. Therefore, we believe that the GCA presented here accounts for interregional temporal variability and directionality, as demonstrated previously (Biswal et al., 2010; Miezin et al., 2000).

While the present study demonstrated the abnormal causal interactions of DLPFC-related circuits in OCD patients, we must note some limitations of this paper. First, BOLD fMRI measures the hemodynamic response changes associated with neuronal activity; it lags a few seconds behind the neuronal responses triggering it. Thus, BOLD fMRI has difficulty detecting neuronal activity that occurs in approximately hundreds of milliseconds. In the future, we need to validate our findings using diverse neuroimaging techniques that detect neuronal activity more directly, including electroencephalography (EEG) and magnetoencephalography (MEG). Second, OCD patients exhibit different types of symptoms, such as checking, reassurance seeking, washing and cleaning rituals, and hoarding (Abramowitz et al., 2009; Fontenelle et al., 2006; McKay et al., 2004). Different symptoms or subtypes may relate to different neural connectivity patterns. In future studies, it will be crucial to collect detailed information about the symptomatic features of OCD subjects for subtype analysis. Third, although we found correlations between EC/FC alterations and symptom severity, the results did not survive Bonferroni correction for multiple comparisons and should be taken with caution. Fourth, we chose only one specific region as the seed in the current study. Given the reliable evidence that large-scale intrinsic network alterations involving multiple brain regions are part of the mechanism of OCD (Gursel et al., 2018), we believe it would be worthwhile to perform GCA on these networks in future studies.

5. Conclusions

To the best of our knowledge, this study is the first to examine the time-directed neural primacy effects on the DLPFC in the resting state in patients with OCD. Our findings extend the neural theory of OCD by specifying the abnormal causal interactions of neural circuits related to the DLPFC in this disorder. We also highlight the directionality of interaction within and between functionally abnormal networks in OCD patients. Further study is needed to investigate whether DLPFC-related FC and EC have the potential to predict treatment outcomes for OCD patients.

CRediT authorship contribution statement

Hailong Li: Conceptualization, Formal analysis, Methodology, Software, Visualization, Writing - original draft, Writing - review & editing. **Xinyu Hu:** Data curation, Formal analysis, Methodology, Software, Validation, Writing - original draft, Writing - review & editing. **Yingxue Gao:** Formal analysis, Methodology, Software, Validation. **Lingxiao Cao:** Formal analysis, Methodology, Validation. **Lianqing Zhang:** Formal analysis, Methodology, Software. **Xuan Bu:** Formal analysis, Methodology, Software. **Lu Lu:** Formal analysis, Methodology, Software. **Yanlin Wang:** Formal analysis, Methodology, Software. **Shi Tang:** Formal analysis, Methodology, Software. **Bin Li:** Data curation, Formal analysis, Supervision. **Yanchun Yang:** Data curation, Formal analysis, Supervision. **Bharat B. Biswal:** Formal analysis, Methodology, Writing - review & editing, Supervision. **Qiyong Gong:** Conceptualization, Data curation, Writing - review & editing, Project administration, Supervision. **Xiaoqi Huang:** Conceptualization, Data curation, Formal analysis, Writing - original draft, Writing - review & editing, Funding acquisition, Project administration, Supervision.

Declaration of Competing Interest

The authors declare that they have no known competing financial interests or personal relationships that could have appeared to influence the work reported in this paper.

Appendix A. Supplementary data

Supplementary data to this article can be found online at https://doi.org/10.1016/j.nicl.2020.102432.

References

Abramowitz, J.S., Taylor, S., McKay, D., 2009. Obsessive-compulsive disorder. Lancet 374, 491–499.

Anticevic, A., Hu, S., Zhang, S., Savic, A., Billingslea, E., Wasylink, S., Repovs, G., Cole, M.W., Bednarski, S., Krystal, J.H., Bloch, M.H., Li, C.S., Pittenger, C., 2014. Global resting-state functional magnetic resonance imaging analysis identifies frontal cortex, striatal, and cerebellar dysconnectivity in obsessive-compulsive disorder. Biol. Psychiatry 75, 595–605.

Biswal, B.B., Eldreth, D.A., Motes, M.A., Rypma, B., 2010. Task-dependent individual differences in prefrontal connectivity. Cereb. Cortex 20, 2188–2197.

Boedhoe, P.S.W., Schmaal, L., Abe, Y., Alonso, P., Ameis, S.H., Anticevic, A., Arnold, P.D., Batistuzzo, M.C., Benedetti, F., Beucke, J.C., Bollettini, I., Bose, A., Brem, S., Calvo, A., Calvo, R., Cheng, Y., Cho, K.I.K., Ciullo, V., Dallaspezia, S., Denys, D., Feusner, J. D., Fitzgerald, K.D., Fouche, J.P., Fridgeirsson, E.A., Gruner, P., Hanna, G.L., Hibar, D.P., Hoexter, M.Q., Hu, H., Huyser, C., Jahanshad, N., James, A., Kathmann, N., Kaufmann, C., Koch, K., Kwon, J.S., Lazaro, L., Lochner, C., Marsh, R., Martinez-Zalacain, I., Mataix-Cols, D., Menchon, J.M., Minuzzi, L., Morer, A., Nakamae, T., Nakao, T., Narayanaswamy, J.C., Nishida, S., Nurmi, E., O'Neill, J., Piacentini, J., Piras, F., Piras, F., Reddy, Y.C.J., Reess, T.J., Sakai, Y., Sato, J.R., Simpson, H.B., Soreni, N., Soriano-Mas, C., Spalletta, G., Stevens, M.C., Szeszko, P.R., Tolin, D.F., van Wingen, G.A., Venkatasubramanian, G., Walitza, S., Wang, Z., Yun, J.Y., Group, E.-O.W., Thompson, P.M., Stein, D.J., van den Heuvel, O.A., Group, E.O.W., 2018. Cortical Abnormalities Associated With Pediatric and Adult Obsessive-Compulsive Disorder: Findings From the ENIGMA Obsessive-Compulsive Disorder Working Group. Am J Psychiatry 175, 453-462.

Bressler, S.L., Menon, V., 2010. Large-scale brain networks in cognition: emerging methods and principles. Trends Cogn. Sci. 14, 277–290.

Curcic-Blake, B., Swart, M., Aleman, A., 2012. Bidirectional information flow in frontoamygdalar circuits in humans: a dynamic causal modeling study of emotional associative learning. Cereb. Cortex 22, 436–445.

de Vries, F.E., de Wit, S.J., Cath, D.C., van der Werf, Y.D., van der Borden, V., van Rossum, T.B., van Balkom, A.J., van der Wee, N.J., Veltman, D.J., van den Heuvel, O.A., 2014. Compensatory frontoparietal activity during working memory: an endophenotype of obsessive-compulsive disorder. Biol. Psychiatry 76, 878–887.

de Wit, S.J., Alonso, P., Schweren, L., Mataix-Cols, D., Lochner, C., Menchon, J.M., Stein, D.J., Fouche, J.P., Soriano-Mas, C., Sato, J.R., Hoexter, M.Q., Denys, D., Nakamae, T., Nishida, S., Kwon, J.S., Jang, J.H., Busatto, G.F., Cardoner, N., Cath, D.C., Fukui, K., Jung, W.H., Kim, S.N., Miguel, E.C., Narumoto, J., Phillips, M.L., Pujol, J., Remijnse, P.L., Sakai, Y., Shin, N.Y., Yamada, K., Veltman, D.J., van den Heuvel, O.A., 2014. Multicenter voxel-based morphometry mega-analysis of structural brain scans in obsessive-compulsive disorder. Am. J. Psychiatry 171, 340–349.

de Wit, S.J., de Vries, F.E., van der Werf, Y.D., Cath, D.C., Heslenfeld, D.J., Veltman, E.M., van Balkom, A.J., Veltman, D.J., van den Heuvel, O.A., 2012. Presupplementary motor area hyperactivity during response inhibition: a candidate endophenotype of obsessive-compulsive disorder. Am. J. Psychiatry 169, 1100–1108.

Del Casale, A., Kotzalidis, G.D., Rapinesi, C., Serata, D., Ambrosi, E., Simonetti, A., Pompili, M., Ferracuti, S., Tatarelli, R., Girardi, P., 2011. Functional neuroimaging in obsessive-compulsive disorder. Neuropsychobiology 64, 61–85.

Dougherty, D.D., Brennan, B.P., Stewart, S.E., Wilhelm, S., Widge, A.S., Rauch, S.L., 2018. Neuroscientifically informed formulation and treatment planning for patients with obsessive-compulsive disorder: a review. JAMA Psychiatry 75, 1081–1087.

Fontenelle, L.F., Mendlowicz, M.V., Versiani, M., 2006. The descriptive epidemiology of obsessive-compulsive disorder. Prog. Neuro-Psychopharmacol. Biol. Psychiatry 30, 327–337.

Friston, K.J., 2011. Functional and effective connectivity: a review. Brain Connect. 1, 13–36.

Fukushima, M., Betzel, R.F., He, Y., de Reus, M.A., van den Heuvel, M.P., Zuo, X.N., Sporns, O., 2018. Fluctuations between high- and low-modularity topology in time-resolved functional connectivity. Neuroimage 180, 406–416.

Guo, W.B., Liu, F., Liu, J.R., Yu, L.Y., Zhang, J., Zhang, Z.K., Xiao, C.Q., Zhai, J.G., Zhao, J.P., 2015. Abnormal causal connectivity by structural deficits in first-episode, drug-naive schizophrenia at rest. Schizophr. Bull. 41, 57–65.

Gursel, D.A., Avram, M., Sorg, C., Brandl, F., Koch, K., 2018. Frontoparietal areas link impairments of large-scale intrinsic brain networks with aberrant fronto-striatal interactions in OCD: a meta-analysis of resting-state functional connectivity. Neurosci. Biobehav. Rev. 87, 151–160.

Hamilton, J.P., Chen, G., Thomason, M.E., Schwartz, M.E., Gotlib, I.H., 2011. Investigating neural primacy in Major Depressive Disorder: multivariate Granger causality analysis of resting-state fMRI time-series data. Mol. Psychiatry 16, 763–772.

Han, H.J., Jung, W.H., Yun, J.Y., Park, J.W., Cho, K.K., Hur, J.W., Shin, N.Y., Lee, T.Y., Kwon, J.S., 2016. Disruption of effective connectivity from the dorsolateral prefrontal cortex to the orbitofrontal cortex by negative emotional distraction in obsessive-compulsive disorder. Psychol. Med. 46, 921–932.

Hilger, K., Fiebach, C.J., 2019. ADHD symptoms are associated with the modular structure of intrinsic brain networks in a representative sample of healthy adults. Netw. Neurosci.. 3, 567–588.

Jiang, Y.C., Luo, C., Li, X., Duan, M.J., He, H., Chen, X., Yang, H., Gong, J.N., Chang, X., Woelfer, M., Biswal, B.B., Yao, D.Z., 2018. Progressive reduction in gray matter in patients with schizophrenia assessed with MR imaging by using causal network analysis (vol 287, pg 633, 2018). Radiology 287, 729.

Kelly, R.M., Strick, P.L., 2003. Cerebellar loops with motor cortex and prefrontal cortex of a nonhuman primate. J. Neurosci. 23, 8432–8444.

Krienen, F.M., Buckner, R.L., 2009. Segregated fronto-cerebellar circuits revealed by intrinsic functional connectivity. Cereb. Cortex 19, 2485–2497.

Kwon, J.S., Jang, J.H., Choi, J.S., Kang, D.H., 2009. Neuroimaging in obsessive-compulsive disorder. Expert Rev. Neurother. 9, 255–269.

Lusicic, A., Schruers, K.R., Pallanti, S., Castle, D.J., 2018. Transcranial magnetic stimulation in the treatment of obsessive-compulsive disorder: current perspectives. Neuropsychiatr. Dis. Treat. 14, 1721–1736.

Mataix-Cols, D., Cullen, S., Lange, K., Zelaya, F., Andrew, C., Amaro, E., Brammer, M.J., Williams, S.C., Speckens, A., Phillips, M.L., 2003. Neural correlates of anxiety associated with obsessive-compulsive symptom dimensions in normal volunteers. Biol. Psychiatry 53, 482–493.

McKay, D., Abramowitz, J.S., Calamari, J.E., Kyrios, M., Radomsky, A., Sookman, D., Taylor, S., Wilhelm, S., 2004. A critical evaluation of obsessive-compulsive disorder subtypes: symptoms versus mechanisms. Clin. Psychol. Rev. 24, 283–313.

Menzies, L., Chamberlain, S.R., Laird, A.R., Thelen, S.M., Sahakian, B.J., Bullmore, E.T., 2008. Integrating evidence from neuroimaging and neuropsychological studies of obsessive-compulsive disorder: the orbitofronto-striatal model revisited. Neurosci. Biobehav. Rev. 32, 525–549.

Meyer-Lindenberg, A., Hariri, A.R., Munoz, K.E., Mervis, C.B., Mattay, V.S., Morris, C.A., Berman, K.F., 2005. Neural correlates of genetically abnormal social cognition in Williams syndrome. Nat. Neurosci. 8, 991–993.

Middleton, F.A., Strick, P.L., 2000a. Basal ganglia and cerebellar loops: motor and cognitive circuits. Brain Res. Brain Res. Rev. 31, 236–250.

Middleton, F.A., Strick, P.L., 2000b. Basal ganglia output and cognition: evidence from anatomical, behavioral, and clinical studies. Brain Cogn. 42, 183–200.

Miezin, F.M., Maccotta, L., Ollinger, J.M., Petersen, S.E., Buckner, R.L., 2000. Characterizing the hemodynamic response: effects of presentation rate, sampling procedure, and the possibility of ordering brain activity based on relative timing. Neuroimage 11, 735–759.

Milad, M.R., Rauch, S.L., 2012. Obsessive-compulsive disorder: beyond segregated cortico-striatal pathways. Trends Cogn. Sci. 16, 43–51.

Moghaddam, B., Homayoun, H., 2008. Divergent plasticity of prefrontal cortex networks. Neuropsychopharmacology 33, 42–55.

Nabeyama, M., Nakagawa, A., Yoshiura, T., Nakao, T., Nakatani, E., Togao, O., Yoshizato, C., Yoshioka, K., Tomita, M., Kanba, S., 2008. Functional MRI study of brain activation alterations in patients with obsessive-compulsive disorder after symptom improvement. Psychiatry Res. 163, 236–247.

Nakao, T., Nakagawa, A., Nakatani, E., Nabeyama, M., Sanematsu, H., Yoshiura, T., Togao, O., Tomita, M., Masuda, Y., Yoshioka, K., Kuroki, T., Kanba, S., 2009. Working memory dysfunction in obsessive-compulsive disorder: a neuropsychological and functional MRI study. J. Psychiatr. Res. 43, 784–791.

Olatunji, B.O., Ferreira-Garcia, R., Caseras, X., Fullana, M.A., Wooderson, S., Speckens, A., Lawrence, N., Giampietro, V., Brammer, M.J., Phillips, M.L., Fontenelle, L.F., Mataix-Cols, D., 2014. Predicting response to cognitive behavioral therapy in contamination-based obsessive-compulsive disorder from functional magnetic resonance imaging. Psychol. Med. 44, 2125–2137.

Palaniyappan, L., Simmonite, M., White, T.P., Liddle, E.B., Liddle, P.F., 2013. Neural primacy of the salience processing system in schizophrenia. Neuron 79, 814–828.

Pezawas, L., Meyer-Lindenberg, A., Drabant, E.M., Verchinski, B.A., Munoz, K.E., Kolachana, B.S., Egan, M.F., Mattay, V.S., Hariri, A.R., Weinberger, D.R., 2005. 5-HTTLPR polymorphism impacts human cingulate-amygdala interactions: a genetic susceptibility mechanism for depression. Nat. Neurosci. 8, 828–834.

Phillips, M.L., Marks, I.M., Senior, C., Lythgoe, D., O'Dwyer, A.M., Meehan, O., Williams, S.C.R., Brammer, M.J., Bullmore, E.T., McGuire, P.K., 2000. A differential neural response in obsessive-compulsive disorder patients with washing compared with checking symptoms to disgust. Psychol. Med. 30, 1037–1050.

Power, J.D., Barnes, K.A., Snyder, A.Z., Schlaggar, B.L., Petersen, S.E., 2013. Steps toward optimizing motion artifact removal in functional connectivity MRI; a reply to Carp. Neuroimage 76, 439–441.

Ramnani, N., 2006. The primate cortico-cerebellar system: anatomy and function. Nat. Rev. Neurosci. 7, 511–522.

Ranganath, C., 2006. Working memory for visual objects: Complementary roles of inferior temporal, medial temporal, and prefrontal cortex. Neuroscience 139, 277–289.

Rehn, S., Eslick, G.D., Brakoulias, V., 2018. A meta-analysis of the effectiveness of different cortical targets used in repetitive transcranial magnetic stimulation (rTMS) for the treatment of obsessive-compulsive disorder (OCD). Psychiatr. Q. 89, 645–665.

Robbins, T.W., Vaghi, M.M., Banca, P., 2019. Obsessive-compulsive disorder: puzzles and prospects. Neuron 102, 27–47.

Rolls, E.T., Cheng, W., Gilson, M., Qiu, J., Hu, Z., Ruan, H., Li, Y., Huang, C.C., Yang, A.C., Tsai, S.J., Zhang, X., Zhuang, K., Lin, C.P., Deco, G., Xie, P., Feng, J., 2018. Effective connectivity in depression. Biol Psychiatry Cogn Neurosci Neuroimaging 3, 187–197.

Russell, A., Cortese, B., Lorch, E., Ivey, J., Banerjee, S.P., Moore, G.J., Rosenberg, D.R., 2003. Localized functional neurochemical marker abnormalities in dorsolateral

prefrontal cortex in pediatric obsessive-compulsive disorder. J. Child Adolesc. Psychopharmacol. 13 (Suppl. 1), S31–38.

Satterthwaite, T.D., Elliott, M.A., Gerraty, R.T., Ruparel, K., Loughead, J., Calkins, M.E., Eickhoff, S.B., Hakonarson, H., Gur, R.C., Gur, R.E., Wolf, D.H., 2013. An improved framework for confound regression and filtering for control of motion artifact in the preprocessing of resting-state functional connectivity data. Neuroimage 64, 240–256.

Savage, C.R., Baer, L., Keuthen, N.J., Brown, H.D., Rauch, S.L., Jenike, M.A., 1999. Organizational strategies mediate nonverbal memory impairment in obsessive-compulsive disorder. Biol. Psychiatry 45, 905–916.

Schippers, M.B., Renken, R., Keysers, C., 2011. The effect of intra- and inter-subject variability of hemodynamic responses on group level Granger causality analyses. Neuroimage 57, 22–36.

Schlosser, R.G.M., Wagner, G., Schachtzabel, C., Peikert, G., Koch, K., Reichenbach, J.R., Sauer, H., 2010. Fronto-cingulate effective connectivity in obsessive compulsive disorder: a study with fMRI and dynamic causal modeling. Hum. Brain Mapp. 31, 1834–1850.

Schmidtke, K., Schorb, A., Winkelmann, G., Hohagen, F., 1998. Cognitive frontal lobe dysfunction in obsessive-compulsive disorder. Biol. Psychiatry 43, 666–673.

Seth, A.K., Barrett, A.B., Barnett, L., 2015. Granger causality analysis in neuroscience and neuroimaging. J. Neurosci. 35, 3293–3297.

Shivakumar, V., Dinakaran, D., Narayanaswamy, J.C., Venkatasubramanian, G., 2019. Noninvasive brain stimulation in obsessive-compulsive disorder. Indian J. Psychiatry 61, S66–S76.

Stein, D.J., Costa, D.L.C., Lochner, C., Miguel, E.C., Reddy, Y.C.J., Shavitt, R.G., van den Heuvel, O.A., Simpson, H.B., 2019. Obsessive-compulsive disorder. Nat. Rev. Dis. Primers 5, 52.

Stein, J.L., Wiedholz, L.M., Bassett, D.S., Weinberger, D.R., Zink, C.F., Mattay, V.S., Meyer-Lindenberg, A., 2007. A validated network of effective amygdala connectivity. Neuroimage 36, 736–745.

Stoodley, C.J., 2012. The cerebellum and cognition: evidence from functional imaging studies. Cerebellum 11, 352–365.

Tang, W., Liu, H., Douw, L., Kramer, M.A., Eden, U.T., Hamalainen, M.S., Stufflebeam, S.M., 2017. Dynamic connectivity modulates local activity in the core regions of the default-mode network. Proc. Natl. Acad. Sci. U.S.A. 114, 9713–9718.

Vaghi, M.M., Vertes, P.E., Kitzbichler, M.G., Apergis-Schoute, A.M., van der Flier, F.E., Fineberg, N.A., Sule, A., Zaman, R., Voon, V., Kundu, P., Bullmore, E.T., Robbins, T.W., 2017. Specific frontostriatal circuits for impaired cognitive flexibility and goal-directed planning in obsessive-compulsive disorder: evidence from resting-state

functional connectivity. Biol. Psychiatry 81, 708–717.

van den Heuvel, O.A., Veltman, D.J., Groenewegen, H.J., Cath, D.C., van Balkom, A.J., van Hartskamp, J., Barkhof, F., van Dyck, R., 2005. Frontal-striatal dysfunction during planning in obsessive-compulsive disorder. Arch. Gen. Psychiatry 62, 301–309.

Xu, T., Zhao, Q., Wang, P., Fan, Q., Chen, J., Zhang, H., Yang, Z., Stein, D.J., Wang, Z., 2019. Altered resting-state cerebellar-cerebral functional connectivity in obsessive-compulsive disorder. Psychol. Med. 49, 1156–1165.

Yan, C.G., Chen, X., Li, L., Castellanos, F.X., Bai, T.J., Bo, Q.J., Cao, J., Chen, G.M., Chen, N.X., Chen, W., Cheng, C., Cheng, Y.Q., Cui, X.L., Duan, J., Fang, Y.R., Gong, Q.Y., Guo, W.B., Hou, Z.H., Hu, L., Kuang, L., Li, F., Li, K.M., Li, T., Liu, Y.S., Liu, Z.N., Long, Y.C., Luo, Q.H., Meng, H.Q., Peng, D.H., Qiu, H.T., Qiu, J., Shen, Y.D., Shi, Y.S., Wang, C.Y., Wang, F., Wang, K., Wang, L., Wang, X., Wang, Y., Wu, X.P., Wu, X.R., Xie, C.M., Xie, G.R., Xie, H.Y., Xie, P., Xu, X.F., Yang, H., Yang, J., Yao, J.S., Yao, S.Q., Yin, Y.Y., Yuan, Y.G., Zhang, A.X., Zhang, H., Zhang, K.R., Zhang, L., Zhang, Z.J., Zhou, R.B., Zhou, Y.T., Zhu, J.J., Zou, C.J., Si, T.M., Zuo, X.N., Zhao, J.P., Zang, Y.F., 2019. Reduced default mode network functional connectivity in patients with recurrent major depressive disorder. Proc. Natl. Acad. Sci. U.S.A. 116, 9078–9083.

Yan, C.G., Cheung, B., Kelly, C., Colcombe, S., Craddock, R.C., Di Martino, A., Li, Q., Zuo, X.N., Castellanos, F.X., Milham, M.P., 2013. A comprehensive assessment of regional variation in the impact of head micromovements on functional connectomics. Neuroimage 76, 183–201.

Yan, C.G., Wang, X.D., Zuo, X.N., Zang, Y.F., 2016. DPABI: Data Processing & Analysis for (Resting-State) Brain Imaging. Neuroinformatics 14, 339–351.

Yucel, M., Harrison, B.J., Wood, S.J., Fornito, A., Wellard, R.M., Pujol, J., Clarke, K., Phillips, M.L., Kyrios, M., Velakoulis, D., Pantelis, C., 2007. Functional and biochemical alterations of the medial frontal cortex in obsessive-compulsive disorder. Arch. Gen. Psychiatry 64, 946–955.

Zald, D.H., Kim, S.W., 1996. Anatomy and function of the orbital frontal cortex, I: anatomy, neurocircuitry; and obsessive-compulsive disorder. J. Neuropsychiatry Clin. Neurosci. 8, 125–138.

Zang, Z.X., Yan, C.G., Dong, Z.Y., Huang, J., Zang, Y.F., 2012. Granger causality analysis implementation on MATLAB: A graphic user interface toolkit for fMRI data processing. J. Neurosci. Methods 203, 418–426.

Zhou, D.D., Wang, W., Wang, G.M., Li, D.Q., Kuang, L., 2017. An updated meta-analysis: Short-term therapeutic effects of repeated transcranial magnetic stimulation in treating obsessive-compulsive disorder. J. Affect. Disord. 215, 187–196.